

Supporting information

P-doping boosting electronic properties and ionic kinetics of MnV_2O_6 for high-performance lithium-ion batteries

Zheng Wu^{§a}, Lang Zhang^{§*a}, Sui Peng^b, Jianhong Yi^a, Dong Fang^{*a}

^aFaculty of Materials Science and Engineering, Kunming University of Science and Technology, Kunming, 650093, China. Email: fangdong@kmust.edu.cn.

^bState Key Laboratory of Vanadium and Titanium Resources Comprehensive Utilization, Panzhihua 61700, China.

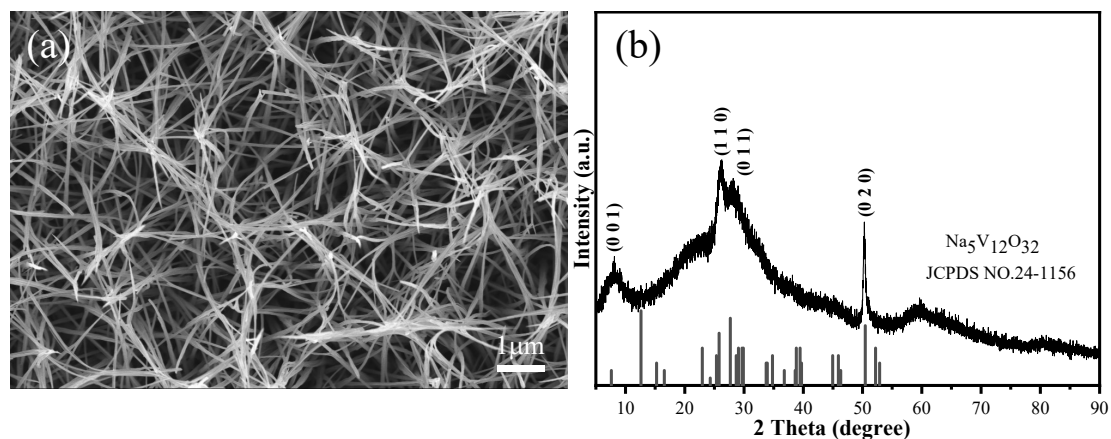


Figure S1 (a) The SEM image and (b) XRD pattern of the $\text{Na}_5\text{V}_{12}\text{O}_{32}$.

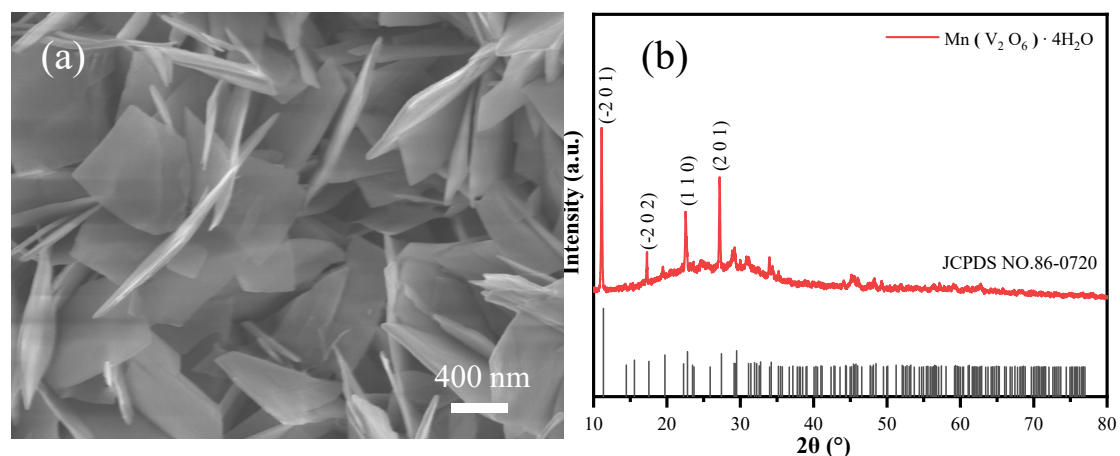


Figure S2 (a) The SEM image and (b) XRD pattern of the $\text{MnV}_2\text{O}_6 \cdot 4\text{H}_2\text{O}$.

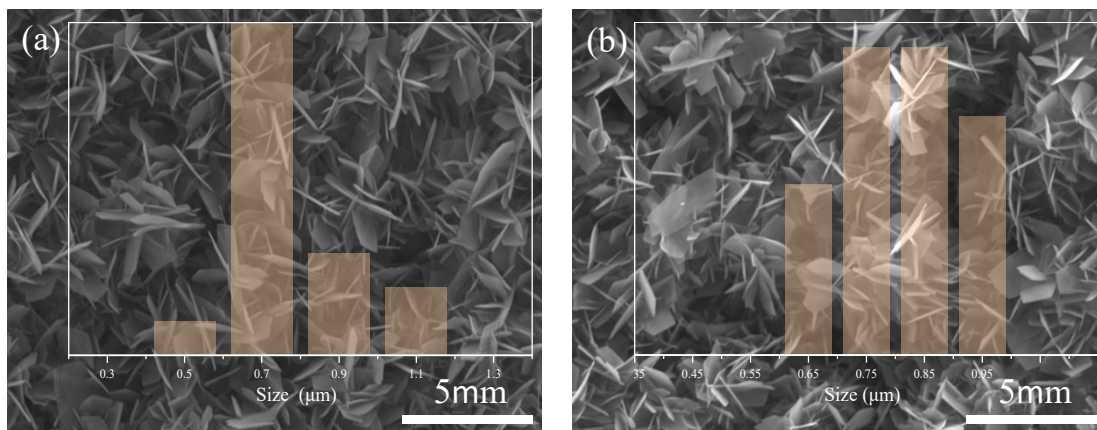


Figure S3 SEM images and the corresponding size statistics of (a) MVO and (b) PMVO.

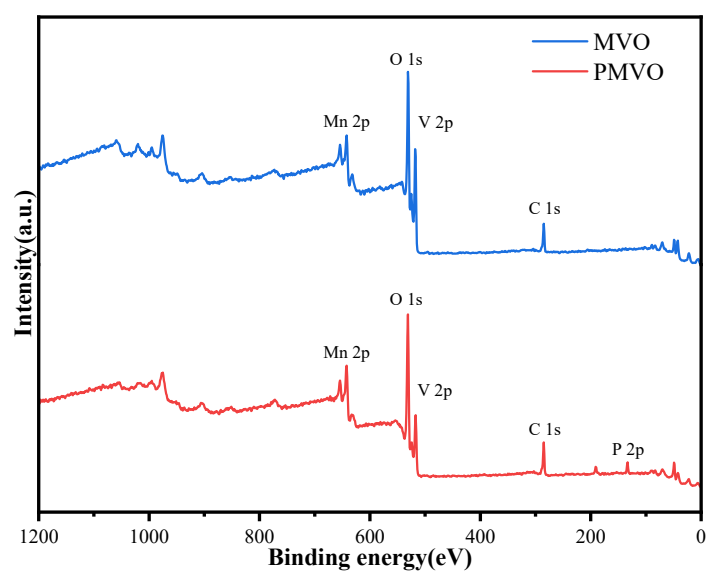


Figure S4 The survey spectra of MVO and PMVO samples.

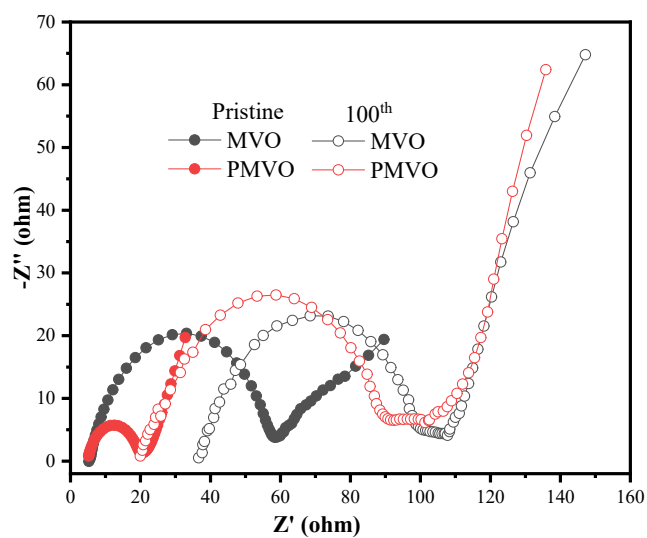


Figure S5 Nyquist plots of MVO and PMVO at pristine state and after cycle to 100 cycles.

Table S1 The R_s and R_{ct} values of MVO and PMVO both pristine state and after cycled 100 times.

	Pristine		100 th	
	R_s (Ω)	R_{ct} (Ω)	R_s (Ω)	R_{ct} (Ω)
MVO	5.59	53.05	36.63	64.12
PMVO	5.20	15.22	19.96	69.53

Table S2 The cell parameters of MVO and PMVO after structural optimization.

	a	b	c	α	β	γ	Volume
MVO	9.704	6.333	7.037	90°	106.713°	90°	414.187
PMVO	9.647	6.252	7.063	90°	108.607°	90°	403.710

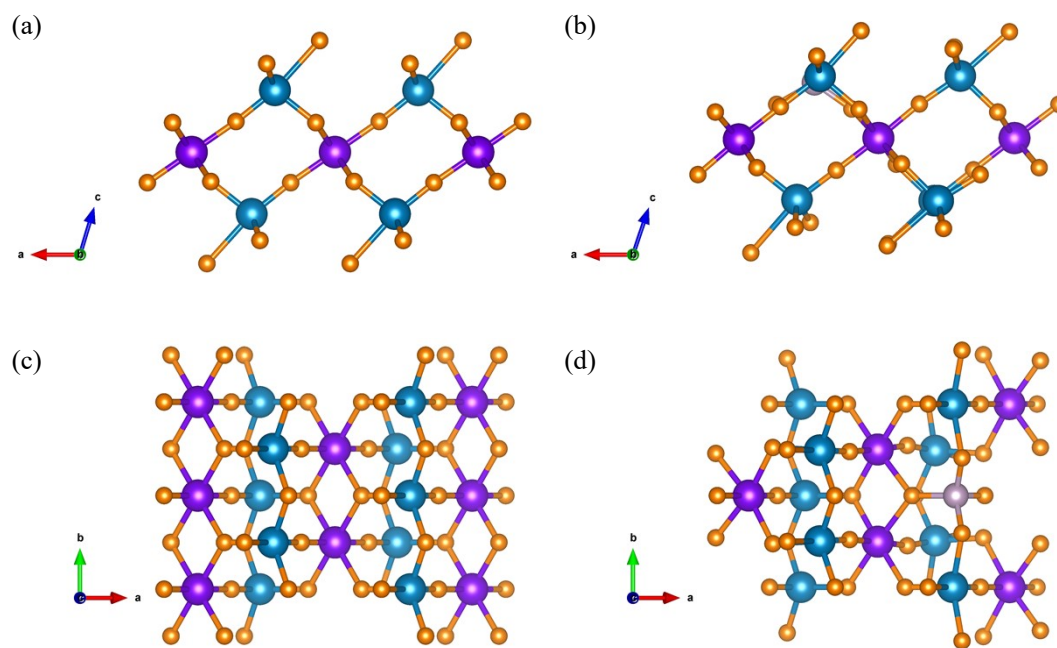


Figure S5 The main views of (a) MVO and (b) PMVO after structural optimization. The top views of (c) MVO and (d) PMVO after structural optimization.

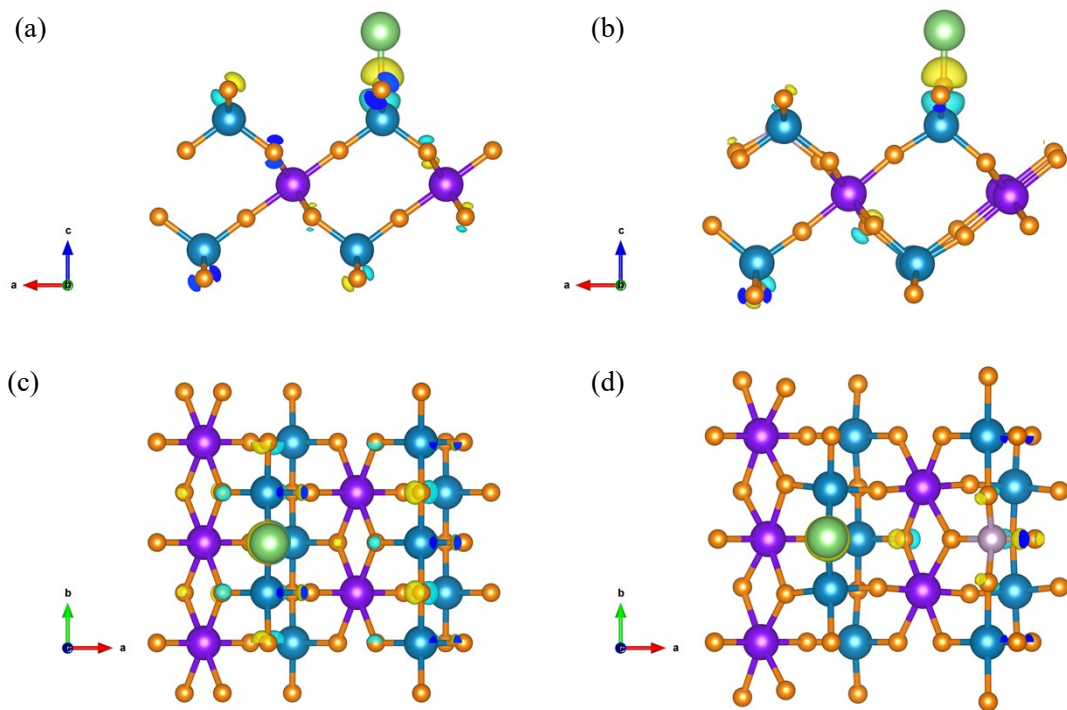


Figure S6 The main views of (a) MVO and (b) PMVO after absorbing one Li^+ . The top views of (c) MVO and (d) PMVO after absorbing one Li^+ .